

Analytic derivative couplings for spin-flip configuration interaction singles and spin-flip time-dependent density functional theory

Xing Zhang and John M. Herbert^{a)}

Department of Chemistry and Biochemistry, The Ohio State University, Columbus, Ohio 43210, USA

(Received 17 May 2014; accepted 22 July 2014; published online 8 August 2014)

We revisit the calculation of analytic derivative couplings for configuration interaction singles (CIS), and derive and implement these couplings for its spin-flip variant for the first time. Our algorithm is closely related to the CIS analytic energy gradient algorithm and should be straightforward to implement in any quantum chemistry code that has CIS analytic energy gradients. The additional cost of evaluating the derivative couplings is small in comparison to the cost of evaluating the gradients for the two electronic states in question. Incorporation of an exchange-correlation term provides an *ad hoc* extension of this formalism to time-dependent density functional theory within the Tamm-Dancoff approximation, without the need to invoke quadratic response theory or evaluate third derivatives of the exchange-correlation functional. Application to several different conical intersections in ethylene demonstrates that minimum-energy crossing points along conical seams can be located at substantially reduced cost when analytic derivative couplings are employed, as compared to use of a branching-plane updating algorithm that does not require these couplings. Application to H₃ near its D_{3h} geometry demonstrates that correct topology is obtained in the vicinity of a conical intersection involving a degenerate ground state. © 2014 AIP Publishing LLC. [<http://dx.doi.org/10.1063/1.4891984>]

I. INTRODUCTION

Most electronic structure methods are based on the Born-Oppenheimer approximation, in which the motions of electrons and nuclei are separated. The nuclei move on an adiabatic potential energy surface (PES), obtained by solving the electronic Schrödinger equation, and the PES is parametrically dependent on the nuclear coordinates. No electronic transitions can be induced by nuclear motion within the Born-Oppenheimer approximation. Nonadiabatic dynamics methods can be applied to go beyond the Born-Oppenheimer approximation,¹ but in order to compute transition probabilities between electronic states, most of these methods require first-order derivative couplings

$$\mathbf{d}^{IJ} = \langle \Psi_I | \hat{\mathbf{V}} | \Psi_J \rangle. \quad (1)$$

These are related to the nonadiabatic coupling vector

$$\mathbf{h}^{IJ} = \langle \Psi_I | (\partial \hat{H} / \partial \mathbf{x}) | \Psi_J \rangle, \quad (2)$$

such that $\mathbf{d}^{IJ} = \mathbf{h}^{IJ} / (E_J - E_I)$, if $|\Psi_I\rangle$ and $|\Psi_J\rangle$ are exact eigenfunctions of the electronic Hamiltonian, \hat{H} . Defining

$$\mathbf{g}^{IJ} = \hat{\mathbf{V}}(E_I - E_J), \quad (3)$$

the vectors \mathbf{g}^{IJ} and \mathbf{h}^{IJ} comprise a basis for the two-dimensional branching space around a two-state conical intersection.² For approximate wave functions, terms in addition to \mathbf{h}^{IJ} arise when evaluating the nuclear derivatives in Eq. (1).³⁻⁶

In principle, \mathbf{h}^{IJ} could be calculated via finite difference, but in the interest of efficiency it is desirable to com-

pute it analytically. This facilitates both nonadiabatic *ab initio* molecular dynamics simulations⁷ as well as optimization of minimum-energy crossing points (MECPs) along conical seams.² The latter are key features in the study of nonadiabatic phenomena in cases where dynamics simulations are not affordable. Analytic formulations of the derivative couplings d_x^{IJ} , where x represents a nuclear coordinate, have been developed and implemented only for a few *ab initio* methods, primarily multireference configuration interaction (MRCI).³⁻⁶ In small molecules, MRCI has the advantages of a fully-balanced treatment of ground and excited states as well as including a large fraction of electron correlation, but its computational cost limits its application to molecules with <20 atoms. Analytic derivative couplings for equation-of-motion coupled-cluster (EOM-CC) theory have been introduced more recently,^{8,9} but EOM-CC methods are also limited to small molecules.

As computationally inexpensive alternatives, analytic derivative couplings for single-reference methods including configuration interaction singles (CIS) and time-dependent density functional theory (TDDFT) have been developed recently.¹⁰⁻¹³ Unfortunately, these methods suffer from an imbalance in the treatment of ground- versus excited-state electron correlation, which makes them suitable only for describing electronic transitions between excited states. This is especially true near the important “funnel” regions along conical seams.¹⁴ For any conical intersection involving the reference state (which is usually the ground state) in CIS or TDDFT, it is readily shown that the branching space is one-dimensional rather than two-dimensional.¹⁴ The same is true, for the same reason, in the case of EOM-CC methods.¹⁵

^{a)}herbert@chemistry.ohio-state.edu

The simplest extensions of CIS and TDDFT that correct these problems are spin-flip (SF) methods: SF-CIS¹⁶ and SF-TDDFT, the latter in its “collinear” formulation.¹⁷ Both of these two methods use a high-spin reference state and compute excitations that include a SF transition, so that, for example, a singlet ground state can be obtained from a self-consistent field (SCF) calculation of a $S_z = 1$ state. Recent computational studies have shown good performance of collinear SF-TDDFT in describing the electronic structure in both Franck-Condon regions and in crossing seam regions.^{19–23}

In the present work, we show that the existing formalism for CIS analytic derivative couplings¹³ can be extended to SF-CIS and (collinear) SF-TDDFT. The resulting equations amount to relatively minor modifications of the CIS or TDDFT analytic gradient formalism, hence computer implementation is straightforward, and the additional cost is modest. Although the extension from CIS to TDDFT is *ad hoc*, numerical examples presented herein demonstrate the accuracy and efficiency of this approach.

II. THEORY

The following notation is used throughout this work. Occupied and virtual molecular spin orbitals are labeled i, j, k, l, \dots and a, b, c, d, \dots , respectively, whereas p, q, r, s, \dots index arbitrary (occupied or virtual) molecular spin orbitals. Greek letters $\mu, \nu, \lambda, \sigma, \dots$ index atomic orbitals. The symbol x represents a nuclear coordinate and derivatives with respect to x will be indicated as, e.g., $\hat{H}^{[x]} = \partial \hat{H} / \partial x$ and $|\Psi_I^{[x]}\rangle = |\partial \Psi_I / \partial x\rangle$. (We use “[x]” to indicate the full derivative with respect to coordinate x , which includes differentiation of the molecular orbitals, rather than a “skeleton derivative,”¹⁸ which does not.) Two-electron integrals are written in physicists’ notation.

A. Analytic derivative couplings for SF-CIS

1. Formalism

In this section, we revisit the analytic formulation of derivative couplings for CIS¹³ and extend it to SF-CIS. (An equation-of-motion formulation of the CIS derivative couplings has appeared recently,²⁴ but we follow the approach in Ref. 13.) The CIS wave function for excited state I is described as a linear combination of singly-excited Slater determinants:

$$|\Psi_I\rangle = \sum_{ai} t_{ai}^I |\Phi_i^a\rangle. \quad (4)$$

For SF-CIS, the Slater determinant $|\Phi_i^a\rangle$ is formed by single $\alpha \rightarrow \beta$ SF excitations from a high-spin Hartree-Fock reference state (e.g., $S_z = 1$ or $S_z = 3/2$) to a low spin target state (e.g., $S_z = 0$ or $S_z = 1/2$).¹⁶ Since spin-conserving CIS calculations use an *ansatz* identical to Eq. (4) but with spin-conserving Slater determinants, we will use the notation $|\Phi_i^a\rangle$ to mean either a spin-conserving or a spin-flipping determinant, depending on whether we wish to consider CIS or SF-CIS. The formalism derived below is valid for both.

The Hellmann-Feynman expression for the derivative coupling is

$$\langle \Psi_I | \Psi_J^{[x]} \rangle = \frac{\langle \Psi_I | \hat{H}^{[x]} | \Psi_J \rangle}{E_J - E_I}. \quad (5)$$

However, this equation holds only when $|\Psi_I\rangle$ and $|\Psi_J\rangle$ are eigenfunctions of \hat{H} . As suggested in Ref. 13, we can use a projection operator

$$\hat{\mathcal{P}} = \sum_{ia} |\Phi_i^a\rangle \langle \Phi_i^a| \quad (6)$$

to project the electronic Hamiltonian \hat{H} onto the single-excitation subspace. Upon subtracting out the Hartree-Fock reference state energy, E_0 , the projected Hamiltonian is defined as

$$\hat{\mathcal{H}} = \hat{\mathcal{P}}(\hat{H} - E_0)\hat{\mathcal{P}}. \quad (7)$$

The CIS wave function in Eq. (4) is an eigenfunction of the model Hamiltonian $\hat{\mathcal{H}}$, with an eigenvalue equal to the CIS excitation energy, ω_I . Thus, the derivative coupling between CIS excited states $|\Psi_I\rangle$ and $|\Psi_J\rangle$ is

$$\langle \Psi_I | \Psi_J^{[x]} \rangle = \frac{\langle \Psi_I | \hat{\mathcal{H}}^{[x]} | \Psi_J \rangle}{\omega_J - \omega_I}. \quad (8)$$

To derive working equations from Eq. (8), we need the derivative of $\hat{\mathcal{H}}$. Using the definition of $\hat{\mathcal{P}}$ we obtain

$$\begin{aligned} \hat{\mathcal{H}}^{[x]} &= \sum_{ijab} [|\Phi_i^a\rangle \langle \Phi_i^a| (\hat{H} - E_0) |\Phi_j^b\rangle \langle \Phi_j^b|]^{[x]} \\ &= \sum_{ijab} (A_{ai,bj} |\Phi_i^{a[x]}\rangle \langle \Phi_j^b| + A_{ai,bj}^{[x]} |\Phi_i^a\rangle \langle \Phi_j^b| \\ &\quad + A_{ai,bj} |\Phi_i^a\rangle \langle \Phi_j^{b[x]}|), \end{aligned} \quad (9)$$

where

$$A_{ai,bj} = \langle \Phi_i^a | (\hat{H} - E_0) | \Phi_j^b \rangle \quad (10)$$

is the matrix element in conventional CIS theory.²⁵ Substituting Eq. (9) into Eq. (8), and using Eq. (4) along with the orthonormality of Slater determinants, we obtain

$$\begin{aligned} (\omega_J - \omega_I) \langle \Psi_I | \Psi_J^{[x]} \rangle &= \sum_{ijab} \langle \Psi_I | \Phi_i^{a[x]} \rangle A_{ai,bj} \langle \Phi_j^b | \Psi_J \rangle \\ &\quad + \sum_{ijab} \langle \Psi_I | \Phi_i^a \rangle A_{ai,bj}^{[x]} \langle \Phi_j^b | \Psi_J \rangle \\ &\quad + \sum_{ijab} \langle \Psi_I | \Phi_i^a \rangle A_{ai,bj} \langle \Phi_j^{b[x]} | \Psi_J \rangle \\ &= \sum_{ijab} \langle \Psi_I | \Phi_i^{a[x]} \rangle A_{ai,bj} t_{bj}^J + \sum_{ijab} t_{ai}^I A_{ai,bj}^{[x]} t_{bj}^J \\ &\quad + \sum_{ijab} t_{ai}^I A_{ai,bj} \langle \Phi_j^{b[x]} | \Psi_J \rangle. \end{aligned} \quad (11)$$

Using the nuclear derivative of the molecular spin-orbitals' creation and annihilation operators,¹³ we next obtain

$$\langle \Psi_I | \Phi_i^{a[x]} \rangle = \sum_c^{\text{particles}} t_{ci}^I \langle c | a^{[x]} \rangle + \sum_k^{\text{holes}} t_{ak}^I \langle k | i^{[x]} \rangle \quad (12)$$

and

$$\langle \Phi_j^{b[x]} | \Psi_J \rangle = \sum_c^{\text{particles}} t_{cj}^J \langle c | b^{[x]} \rangle + \sum_k^{\text{holes}} t_{bk}^J \langle k | j^{[x]} \rangle. \quad (13)$$

Next, recall that the CIS equations for states I and J are

$$\begin{aligned} \sum_{ia} t_{ai}^I A_{ai,bj} &= \omega_I t_{bj}^I, \\ \sum_{jb} A_{ai,bj} t_{bj}^J &= \omega_J t_{ai}^J. \end{aligned} \quad (14)$$

Combining Eq. (14) with the results above, we obtain a general expression for the derivative coupling that is valid for both spin-conserved and spin-flip CIS,

$$\begin{aligned} (\omega_J - \omega_I) \langle \Psi_I | \Psi_J^{[x]} \rangle &= \sum_{ac} \sum_i (t_{ci}^I t_{ai}^J \omega_J + t_{ci}^J t_{ai}^I \omega_I) \langle c | a^{[x]} \rangle \\ &+ \sum_{ik} \sum_a (t_{ak}^I t_{ai}^J \omega_J + t_{ak}^J t_{ai}^I \omega_I) \langle k | i^{[x]} \rangle \\ &+ \sum_{ijab} t_{ai}^I A_{ai,bj}^{[x]} t_{bj}^J. \end{aligned} \quad (15)$$

Overlap integrals between virtual orbitals and their displaced counterparts are given by

$$\langle c | a^{[x]} \rangle = \sum_{\mu\nu} C_{\mu c} \langle \mu | v^{[x]} \rangle C_{\nu a} + \sum_{\mu\nu} C_{\mu c} \langle \mu | v \rangle C_{\nu a}^{[x]}. \quad (16)$$

The derivatives $C_{\nu a}^{[x]}$ of the molecular orbital (MO) coefficients can be expanded in the unperturbed MO basis,²⁶

$$C_{\nu a}^{[x]} = \sum_p^{\text{all}} C_{\nu p} U_{pa}^{[x]}. \quad (17)$$

The virtual–virtual coefficients $U_{ba}^{[x]}$ are redundant, and can be expressed as¹⁸

$$U_{ba}^{[x]} = -\frac{1}{2} S_{ba}^{[x]}, \quad (18)$$

where

$$S_{ba}^{[x]} = \sum_{\mu\nu} C_{\mu b} S_{\mu\nu}^{[x]} C_{\nu a} \quad (19)$$

is a so-called skeleton derivative¹⁸ of a MO overlap integral, meaning that it is evaluated for fixed MO coefficients. In contrast, the quantity $S_{\mu\nu}^{[x]} = \partial \langle \mu | v \rangle / \partial x$ is simply an overlap derivative in the atomic orbital (AO) basis. Equation (19) follows from the fact that $\mathbf{U}^{[x]} + (\mathbf{U}^{[x]})^\dagger = -\mathbf{S}^{[x]}$.

Putting all of this together, we have

$$C_{\nu a}^{[x]} = \sum_i^{\text{occ}} C_{\nu i} U_{ia}^{[x]} - \frac{1}{2} \sum_b^{\text{virt}} C_{\nu b} S_{ba}^{[x]}. \quad (20)$$

However, the term involving $U_{ia}^{[x]}$ vanishes when this equation is inserted into Eq. (16), because $\langle c | i \rangle = 0$, and thus $\langle c | a^{[x]} \rangle$ can be evaluated without the need to solve coupled-perturbed equations. Instead, we obtain

$$\begin{aligned} \langle c | a^{[x]} \rangle &= \sum_{\mu\nu} C_{\mu c} \langle \mu | v^{[x]} \rangle C_{\nu a} \\ &- \frac{1}{2} \sum_{\mu\nu} \sum_d^{\text{virt}} C_{\mu c} \langle \mu | v \rangle C_{\nu d} S_{da}^{[x]}. \end{aligned} \quad (21)$$

A similar expression can be derived for the terms $\langle k | i^{[x]} \rangle$ that appear in Eq. (15):

$$\begin{aligned} \langle k | i^{[x]} \rangle &= \sum_{\mu\nu} C_{\mu k} \langle \mu | v^{[x]} \rangle C_{\nu i} \\ &- \frac{1}{2} \sum_{\mu\nu} \sum_j^{\text{occ}} C_{\mu k} \langle \mu | v \rangle C_{\nu j} S_{ji}^{[x]}. \end{aligned} \quad (22)$$

2. Discussion

Equation (15) is a compact expression for the CIS derivative couplings. The non-Hellman–Feynman (or “response”) terms in this expression are easily evaluated using Eqs. (21) and (22), while the Hellman–Feynman term is analogous to the conventional CIS energy gradient expression,²⁷

$$\omega_I^{[x]} = \sum_{ijab} t_{ai}^I A_{ai,bj}^{[x]} t_{bj}^I, \quad (23)$$

but with different excitation eigenvectors on the right and left in Eq. (15). As such, we can calculate CIS analytic derivative couplings using the same algorithm for as for CIS analytic energy gradients,^{27,28} and very little extra coding is required. Actually, our Eq. (15) for the derivative couplings is equivalent to Eq. (A23) in Ref. 13, although our derivation is somewhat more compact. Our algorithm is also analogous to that used to compute analytic derivative couplings for MRCI wave functions,^{3–6} where the Hellman–Feynman term is sometimes called the “CI contribution” and the non-Hellman–Feynman terms are the “configuration state function (CSF) contribution.”²⁶ Following the convention in MRCI, we identify only the Hellman–Feynman contribution as the nonadiabatic coupling

$$h_x^{IJ} = \sum_{ijab} t_{ai}^I A_{ai,bj}^{[x]} t_{bj}^J. \quad (24)$$

Because we have only approximate wave functions in CIS theory, the nonadiabatic coupling is *not* simply equal to \mathbf{d}^{IJ} times the energy gap, i.e., the relationship between Eqs. (1) and (2) is not respected.

The explicit form of $A_{ai,bj}^{[x]}$ is derived in the Appendix. Note also that the wave function *ansatz* in Eq. (4) is invariant to unitary transformations of the occupied orbitals and, separately, to unitary transformations of the virtual orbitals, hence Eq. (15) for the derivative couplings is also invariant to such transformations.

A long-known problem with derivative couplings, but one that is sometimes overlooked, is their lack of translational invariance.^{3,29–32} In a nonadiabatic dynamics

simulation, this allows constant-velocity motion of the entire system to stimulate transitions between adiabatic electronic states, behavior that is ultimately an artifact of using real-valued Born-Oppenheimer electronic states for the coupled electron–nuclear dynamics.^{13,29} Motivated by earlier literature on atom–atom scattering calculations,²⁹ Fatehi *et al.*^{13,32} recently introduced electron translation factors (ETFs) for analytic derivative couplings computed using atom-centered basis sets. These authors suggest that the magnitude of the ETFs may be significant for high-symmetry molecules.³²

ETFs are intended to restore translational invariance in the nonadiabatic nuclear dynamics. This can be realized by introducing complex phase factors into the AO basis functions,¹³ which allow the electrons to propagate alongside the nuclei and which render the nonadiabatic equations of motion rigorously translationally invariant. To achieve this, the CIS derivative coupling that appears in the equations of motion is replaced by a ETF-corrected derivative coupling of the form¹³

$$\langle \Psi_I | \Psi_J^{[x]} \rangle_{\text{ETF}} = \langle \Psi_I | \Psi_J^{[x]} \rangle + \sum_{\mu\nu} \tilde{S}_{\mu\nu}^{[x]} \left(\sum_{iab} C_{va} t_{ai}^I t_{bi}^J C_{\mu b} + \sum_{ija} C_{vi} t_{ai}^I t_{aj}^J C_{\mu j} \right), \quad (25)$$

where

$$\tilde{S}_{\mu\nu}^{[x]} = \frac{1}{2} (\langle \mu | v^{[x]} \rangle - \langle v | \mu^{[x]} \rangle). \quad (26)$$

Interestingly, it is easy to show that the first two terms in Eq. (15) can be rewritten as

$$\begin{aligned} & \sum_{ac} \sum_i (t_{ci}^I t_{ai}^J \omega_J + t_{ci}^J t_{ai}^I \omega_I) \langle c | a^{[x]} \rangle \\ & + \sum_{ik} \sum_a (t_{ak}^I t_{ai}^J \omega_J + t_{ak}^J t_{ai}^I \omega_I) \langle k | i^{[x]} \rangle \\ & = (\omega_I - \omega_J) \sum_{\mu\nu} \tilde{S}_{\mu\nu}^{[x]} \left(\sum_{iab} C_{va} t_{ai}^I t_{bi}^J C_{\mu b} + \sum_{ija} C_{vi} t_{ai}^I t_{aj}^J C_{\mu j} \right). \end{aligned} \quad (27)$$

Thus, the ETF-corrected derivative coupling in Eq. (25) is actually identical to the final term in Eq. (15),

$$\langle \Psi_I | \Psi_J^{[x]} \rangle_{\text{ETF}} = (\omega_J - \omega_I)^{-1} \sum_{ijab} t_{ai}^I A_{ai,bj}^{[x]} t_{bj}^J. \quad (28)$$

In other words, the ETF correction precisely cancels the non-Hellman–Feynman terms in the expression for the derivative coupling!

Within CIS theory, the elements h_x^{IJ} of the nonadiabatic coupling vector are

$$h_x^{IJ} = (\omega_J - \omega_I) \langle \Psi_I | \Psi_J^{[x]} \rangle_{\text{ETF}}. \quad (29)$$

Thus, we find that the ETF-corrected derivative couplings in CIS theory may actually be more useful than the full derivative couplings formulated in Eq. (15). This observation may have implications in the context of derivative couplings for

non-variational, correlated wave function methods such as EOM-CC.⁹

B. Analytic derivative couplings for SF-TDDFT

SF-TDDFT (with a collinear spin density) was originally introduced by Shao *et al.*¹⁷ Unlike the conventional linear-response TDDFT, and also unlike SF-TDDFT with a non-collinear spin density,³³ collinear SF-TDDFT resembles a modified SF-CIS *ansatz* wherein Kohn-Sham MOs and the Kohn-Sham effective Hamiltonian are used in place of their Hartree-Fock counterparts. We therefore propose an *ad hoc* modification to the CIS formalism, in which matrix elements $\langle \Phi_i^a | \hat{H} | \Phi_j^b \rangle$ are replaced by their TDDFT counterparts. The latter are given by

$$\langle \Phi_i^a | \hat{H}_{\text{KS}} | \Phi_j^b \rangle = E_{\text{KS}} \delta_{ij} \delta_{ab} + f_{ab} \delta_{ij} - f_{ij} \delta_{ab} + \langle aj | ib \rangle - C_{\text{HF}} \langle aj | bi \rangle + \langle aj | \hat{\xi}_{\text{xc}} | ib \rangle, \quad (30)$$

where E_{KS} is the Kohn-Sham SCF energy, \hat{f} is the Kohn-Sham Fock operator, C_{HF} is the fraction of Hartree-Fock exchange in the exchange-correlation functional, and

$$\langle aj | \hat{\xi}_{\text{xc}} | ib \rangle = \int d\mathbf{r} d\mathbf{r}' \phi_a(\mathbf{r}) \phi_i(\mathbf{r}) \frac{\delta^2 f_{\text{xc}}}{\delta \rho(\mathbf{r}) \delta \rho(\mathbf{r}')} \phi_b(\mathbf{r}') \phi_j(\mathbf{r}') \quad (31)$$

is a matrix element of the exchange-correlation kernel. From Eq. (30), it is clear that Eqs. (15), (28), and (29) are valid for collinear SF-TDDFT except that the matrix elements $A_{ai,bj}^{[x]}$ must be modified according to the SF-TDDFT analytic energy gradient.¹⁷ Details are shown in the Appendix.

Effectively, we are “grafting on” an exchange-correlation term to SF-CIS, which at some level amounts to taking seriously the Kohn-Sham determinant as a wave function and will need to be validated with benchmark studies. Ou *et al.*³⁴ recently introduced derivative couplings for spin-conserving TDDFT within the Tamm-Dancoff approximation (TDA),³⁵ based on the same *ad hoc* modification applied to a version of Eq. (15). There is some evidence that the TDA may be better suited for exploration of potential energy surfaces, as compared to full TDDFT, owing to triplet instabilities in the latter method.³⁶

III. NUMERICAL EXAMPLES

Both Eq. (15) for $\langle \Psi_I | \Psi_J^{[x]} \rangle$, as well as Eq. (28) for the ETF-corrected derivative coupling, have been implemented in a locally modified version of the Q-CHEM program,^{37,38} for both spin-conserved CIS, spin-flip CIS, and collinear SF-TDDFT. For the spin-conserving cases, both spin-restricted and unrestricted reference states have been implemented, though a restricted open-shell reference is not yet implemented. Finite-difference results are in excellent agreement with the analytic implementations of all three methods (see the supplementary material³⁹), which is compelling evidence of the validity of our implementation. In addition, the derivative couplings computed using Eqs. (15) and (28) are exactly the same as the corresponding couplings computed using the formalism introduced in Ref. 13 for spin-conserved

CIS, which was implemented in Q-CHEM by the authors of Ref. 13. This agreement is not surprising, since the two approaches are formally equivalent for spin-conserved CIS, but provides additional evidence in support of the correctness of our implementation. Illustrative numerical examples of the new SF-CIS and SF-TDDFT derivative couplings are presented below.

A. H_3 potential surfaces near a conical intersection

Levine *et al.*¹⁴ have shown that spin-conserved CIS and TDDFT cannot provide correct topology of the PES in the vicinity of a conical intersection that involves the reference state (usually the ground state), and numerical examples have been presented.^{14,40} This is mainly due to the single-excitation nature of spin-conserved CIS and TDDFT as well as the unbalanced treatment of ground and excited states. For CIS calculations, the combination of this imbalance along with Brillouin's theorem means that the CIS method fails to provide a correct description of degenerate ground states.

SF-CIS and SF-TDDFT, on the other hand, can provide correct PESs near conical intersections, because these methods contain some determinants that look like double excitations relative to the ground state. Thus, the ground state is treated on a more balanced footing with respect to the excited states. In other words, conical intersections with double-excitation character (e.g., twisted-pyramidalized ethylene¹⁹) can be described by SF-CIS and SF-TDDFT, and there is fur-

thermore no fundamental problem in describing a degenerate ground state.

Our first test system is H_3 in D_{3h} symmetry, which requires the D_0 and D_1 states to be degenerate, and we will compare SF-CIS and collinear SF-TDDFT results to restricted open-shell CIS (ROCIS) and spin-conserving TDA-TDDFT. In this particular case, spin-conserving, unrestricted CIS fails to describe this system due to significant spin contamination, necessitating the use of a restricted open-shell reference state. Furthermore, spin-conserving TDDFT fails in the presence of the near-degeneracy, owing to imaginary roots (triplet instabilities) in the orbital Hessian. For this reason, the spin-conserving TDDFT calculations were performed within the TDA. The latter calculations employ the B3LYP functional, while SF-TDDFT calculations employ the BH&HLYP functional (50% Hartree-Fock exchange plus 50% Becke exchange⁴¹ with Lee-Yang-Parr correlation⁴²), and we abbreviate this method as SF-BH&HLYP.

We scanned over the bond length of all D_{3h} geometries for H_3 , using the 6-31G* basis set for all energy scans, finding minimum-energy conical intersections at $R = 1.35 \text{ \AA}$ (SF-CIS), $R = 1.19 \text{ \AA}$ (SF-BH&HLYP), $R = 1.09 \text{ \AA}$ (ROCIS), and $R = 1.09 \text{ \AA}$ (TD-B3LYP). In Fig. 1, two internal coordinates (one angle and one bond length, as shown in the figure) are varied to depict the PES in the vicinity of the D_{3h} conical intersection.

The degeneracy between the D_0 and D_1 states does not appear for most equilateral triangular geometries in ROCIS calculations because the D_0 and D_1 states are calculated within different schemes (i.e., Hartree-Fock SCF versus

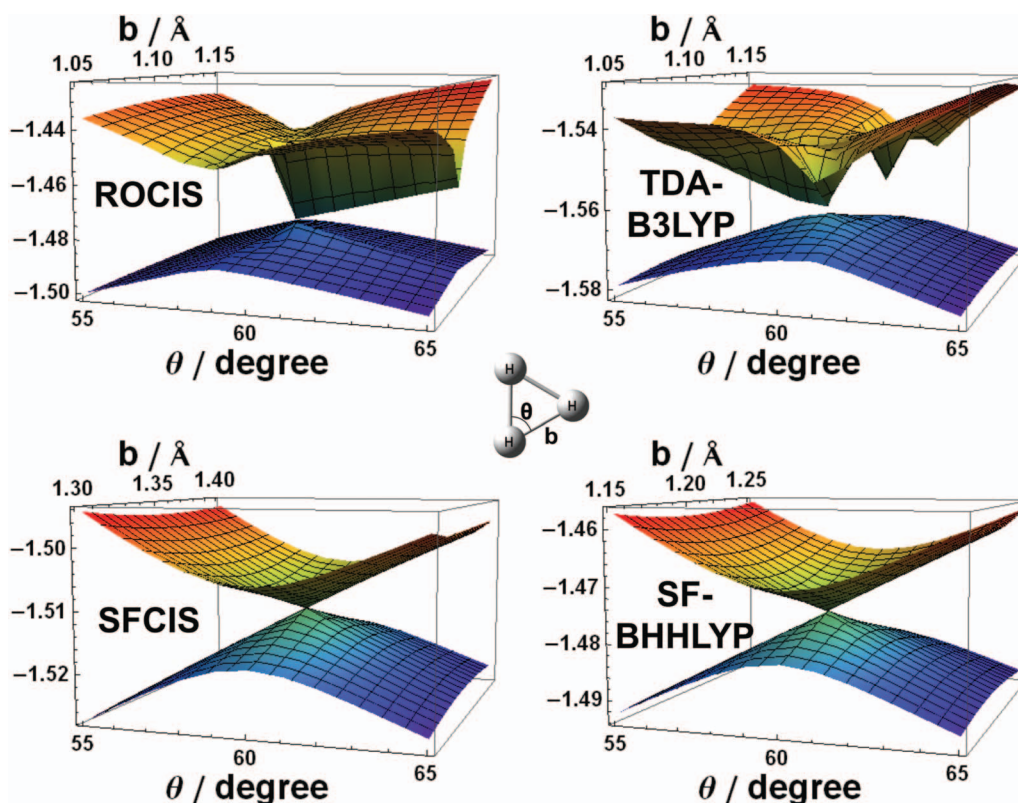


FIG. 1. Potential energy surfaces around the conical intersections of D_{3h} H_3 calculated by restricted open-shell CIS, unrestricted TD-B3LYP within the Tamm-Dancoff approximation, SF-CIS, and SF-BH&HLYP. All calculations employ the 6-31G* basis set, and energies are shown in atomic units.

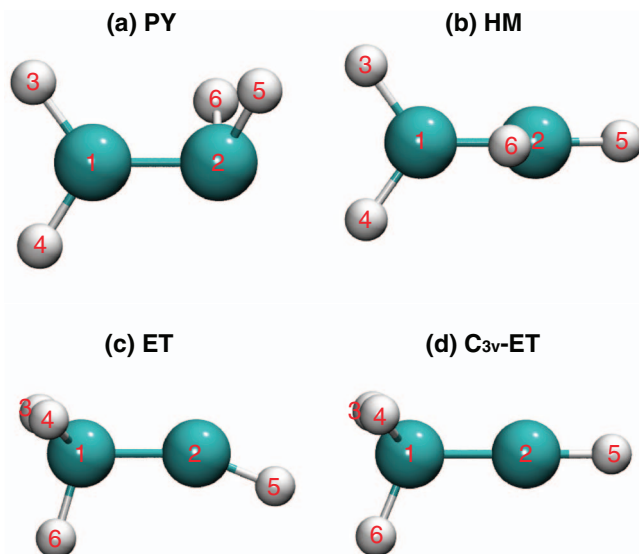


FIG. 2. Geometries for the MECPs of ethylene: (a) twisted-pyramidalized (PY), (b) hydrogen-migration (HM), (c) ethylidene (ET), and (d) C_{3v} ethylidene (C_{3v}-ET).

configuration interaction). Moreover, the D₁ surface shows an unphysical sharp cusp near the intersection. This has been observed in spin-conserving TDDFT calculations as well,¹⁴ and is confirmed by the TDA-B3LYP results in Fig. 1, wherein D₁ exhibits multiple, unphysical cusps. SF-CIS and SF-BH&HLYP calculations, on the other hand, clearly provide the correct double-cone shape, and the surface varies smoothly away from the intersection.

Although this particular symmetry-required degeneracy between doublet states is correctly reproduced by SF-CIS and SF-TDDFT, not all possible single and double excitations are contained in the SF set of excitations, and as such there certainly exist systems where a degenerate ground state is not correctly reproduced by these methods. For example, SF-CIS and SF-BH&HLYP fail to produce the symmetry-required degeneracy in linear H–O–H (D_{∞h} symmetry). Symmetry-required degeneracies that involve the ground state (e.g., Jahn-Teller problems) may be problematic in general for these methods, as significant spin contamination can lead to

TABLE II. Relative energies (in eV) for the four critical points of ethylene that are depicted in Fig. 2, as calculated at the SF-CIS/6-31G(d,p), SF-BH&HLYP/6-31G(d,p), and MR-CISD/aug'-cc-pVTZ levels. (MRCI values are taken from Ref. 43.)

MECP	SF-CIS		SF-BH&HLYP		MRCI	
	S ₀	S ₁	S ₀	S ₁	S ₀	S ₁
S _{0min}	0.00	9.07	0.00	8.35	0.00	8.02
PY	5.88	5.88	4.85	4.85	4.83	4.83
HM	6.51	6.51	5.49	5.49	5.38	5.38
ET	4.71	4.71	4.62	4.62	4.49	4.49
C _{3v} -ET	4.86	4.86	4.70	4.70	4.59	4.60

a lifting of what should properly be a symmetry-imposed degeneracy.

B. Minimum-energy crossing points for ethylene

In contrast to the symmetry-imposed degeneracy in H₃, we next consider some accidental degeneracies in ethylene. We have used SF-CIS and SF-TDDFT to locate four critical points (see Fig. 2) on the S₀/S₁ crossing seam, for which we can compare our results to a previous MRCI study.⁴³ Three of these critical points are local MECPs, whereas structure **HM** in Fig. 2 is actually a saddle point on the crossing seam.⁴³ Critical points were optimized using the projected-gradient algorithm of Bearpark *et al.*,⁴⁴ which involves optimizing along the gradient

$$\mathbf{g} = 2(E_J - E_I)\mathbf{x} + \mathbf{P}\mathbf{g}_{\text{mean}}. \quad (32)$$

The quantity

$$\mathbf{g}_{\text{mean}} = \frac{1}{2}\hat{\nabla}(E_I + E_J) \quad (33)$$

is the average energy gradient for states *I* and *J*,

$$\mathbf{x} = \frac{\hat{\nabla}(E_J - E_I)}{\|\hat{\nabla}(E_J - E_I)\|} \quad (34)$$

is the normalized gradient difference vector, and

$$\mathbf{P} = \mathbf{1} - \mathbf{xx}^\dagger - \mathbf{yy}^\dagger \quad (35)$$

TABLE I. Geometric parameters for the four ethylene critical points depicted in Fig. 2, optimized by SF-CIS/6-31G(d,p), SF-BH&HLYP/6-31G(d,p), and MR-CISD/aug'-cc-pVTZ levels. (MRCI values are taken from Ref. 43.)

Parameter	PY			HM			ET			C _{3v} -ET		
	Spin-flip			Spin-flip			Spin-flip			Spin-flip		
	CIS	BH&HLYP	MRCI	CIS	BH&HLYP	MRCI	CIS	BH&HLYP	MRCI	CIS	BH&HLYP	MRCI
C ₁ -C ₂	1.415	1.384	1.399	1.363	1.338	1.360	1.452	1.434	1.448	1.456	1.437	1.452
C ₂ -H ₅	1.082	1.098	1.096	1.054	1.056	1.063	1.056	1.060	1.068	1.050	1.056	1.064
C ₂ -H ₆	1.209	1.140	1.163	1.231	1.162	1.180						
C ₁ -H ₃	1.089	1.098	1.098	1.092	1.108	1.105	1.090	1.094	1.096	1.090	1.095	1.097
∠C ₁ C ₂ H ₅	123.6	113.4	118.6	168.9	162.1	164.1	156.3	157.3	155.1			
∠C ₁ C ₂ H ₆	66.9	89.7	82.8	62.7	75.5	72.8						
∠H ₅ C ₂ H ₆	98.3	92.2	94.4	128.4	122.5	121.9						
∠H ₃ C ₁ C ₂ H ₅	23.1	39.3	35.2	-88.1	-93.7	-76.3						
∠H ₄ C ₁ C ₂ H ₆	108.0	120.0	114.7	-89.7	-85.5	-88.1						

TABLE III. Efficiencies of two different algorithms for locating ethylene MECPs, at the SF-BH&HLYP/6-31G** level. The same convergence criteria and starting structures were used for both algorithms.

MECP	Using \mathbf{g} only ^a		Using \mathbf{g} and \mathbf{h}^b	
	Iterations	time/s	Iterations	time/s
PY	49	1126	21	566
ET	20	429	8	201

^aBranching-plane updating method of Ref. 45.

^bProjected-gradient method of Ref. 44.

projects out the vector \mathbf{x} and also the vector

$$\mathbf{y} = \frac{(\mathbf{1} - \mathbf{xx}^\dagger)\mathbf{h}^{IJ}}{\|(\mathbf{1} - \mathbf{xx}^\dagger)\mathbf{h}^{IJ}\|} \quad (36)$$

from the mean gradient.

Some selected internal coordinates were compared with the MRCI results in Table I. The SF-BH&HLYP and MRCI geometries are in good agreement, and the SF-CIS geometries agree qualitatively with the MRCI results, except that for the **PY** and **HM** structures optimized by SF-CIS, the extent of hydrogen migration is slightly overestimated as compared with the SF-BH&HLYP and MRCI results.

The relative energies of the four critical points are shown in Table II. SF-BH&HLYP energies agree well with the MRCI results in all four cases. However, SF-CIS energies differ by more than 1 eV (as compared to the MRCI energies) for S_{0min} , **PY**, and **HM**. This likely reflects the lack of dynamical correlation in SF-CIS.

Finally, we compare the efficiency of the aforementioned projected-gradient optimization algorithm,⁴⁴ which uses both \mathbf{g}^{IJ} and \mathbf{h}^{IJ} , to that of a branching-plane updating algorithm⁴⁵ that requires only \mathbf{g}^{IJ} . (We find the latter algorithm to be much more efficient as compared to penalty-constrained approaches⁴⁶ that also do not require derivative couplings.) Performance data for ethylene MECPs are shown in Table III, from which we see that the branching-plane updating algorithm requires more than twice as many iterations to converge as compared to the projected-gradient algorithm. Calculation of \mathbf{h}^{IJ} adds only a very small cost per iteration, hence the projected-gradient algorithm based on analytic derivative couplings affords significantly faster timings.

IV. SUMMARY

We have formulated and implemented analytic first derivative couplings for SF-CIS, which are simple extensions of previous work on derivative couplings for spin-conserved CIS but have the advantage that the SF methods describe ground and excited states in a more balanced way. *Ad hoc* introduction of an exchange-correlation term in the Hamiltonian then affords derivative couplings for (collinear) SF-TDDFT. Numerical examples demonstrate that these SF methods provide correct topologies in the vicinity of conical intersections and reasonable energetics across the PES, as we saw in a previous study as well.²³ As such, these methods seem like good choices for nonadiabatic *ab initio* molecular dynamics simulations, especially in the case of SF-TDDFT, which incor-

porates dynamical electron correlation. (Static correlation is handled via the SF formalism.)

Although spin contamination becomes problematic for some systems,²³ these SF methods can in principle be extended to their spin-complete counterparts.^{47–49} The SF-extended CIS method,⁴⁹ for example, is the spin-complete version of SF-CIS, and analytic derivative couplings can be derived without difficulty using the formalism described here. Collinear SF-TDDFT can be similarly extended, and a restricted open-shell formulation is also possible but has not yet been implemented. Finally, it is straightforward to extend our formalism to evaluate derivative couplings for *non-collinear* SF-TDDFT within the TDA,³³ as the analytic gradient of this method has recently been reported.⁵⁰ Extensions along these lines are currently in progress in our group.

ACKNOWLEDGMENTS

This work was supported by the National Science Foundation (CHE-1300603) and calculations were performed at the Ohio Supercomputer Center under project PAA-0003. J.M.H. is an Alfred P. Sloan Foundation fellow and a Camille Dreyfus Teacher-Scholar. We thank Professor Joe Subotnik for providing a preprint of Ref. 34.

APPENDIX: DETAILED DERIVATIONS

1. Derivation of h_x^{IJ} for SF-CIS

Following the formalism of the CIS analytic energy gradient,^{27,28} the nonadiabatic coupling vector h_x^{IJ} in Eq. (29) can be expressed as

$$\begin{aligned} h_x^{IJ} &= \sum_{ijab} t_{ai}^I A_{ai,bj}^{[x]} t_{bj}^J \\ &= \sum_{ijab} t_{ai}^I (F_{ab}^{[x]} \delta_{ij} - F_{ij}^{[x]} \delta_{ab} + \langle a|j||i|b\rangle^{[x]}) t_{bj}^J, \end{aligned} \quad (A1)$$

where F_{ij} and F_{ab} are Fock matrix elements. Hereafter, we will use matrix notation for simplicity.⁵¹ Matrix elements of the Fock operator are

$$F_{\mu\nu} = \langle \mu | \hat{f} | \nu \rangle \quad (A2)$$

and its one-electron part is

$$H_{\mu\nu} = \langle \mu | \hat{h} | \nu \rangle, \quad (A3)$$

whereas two-electron integrals are denoted

$$\Pi_{\mu\nu,\lambda\sigma} = \langle \mu\lambda || \nu\sigma \rangle. \quad (A4)$$

The overlap matrix is

$$S_{\mu\nu} = \langle \mu | \nu \rangle \quad (A5)$$

and

$$P_{\mu\nu} = \sum_k^{\text{occ}} C_{\mu k} C_{\nu k} \quad (A6)$$

is the one-electron density matrix. The difference density matrix for the excited state is

$$\mathbf{P}^\Delta = \frac{1}{2}\mathbf{C}_v(\mathbf{t}^I\mathbf{t}^{J\dagger} + \mathbf{t}^J\mathbf{t}^{I\dagger})\mathbf{C}_v^\dagger - \frac{1}{2}\mathbf{C}_0(\mathbf{t}^I\mathbf{t}^J + \mathbf{t}^J\mathbf{t}^I)\mathbf{C}_0^\dagger, \quad (\text{A7})$$

where \mathbf{C}_0 and \mathbf{C}_v are rectangular matrices containing the occupied and virtual MO coefficients, respectively.

Next, define

$$\mathbf{R}^I = \mathbf{C}_v\mathbf{t}^I\mathbf{C}_0^\dagger \quad (\text{A8})$$

for state I , with a similar quantity \mathbf{R}^J for state J , and

$$\mathbf{P}^Z = \mathbf{C}_v\mathbf{Z}\mathbf{C}_0^\dagger + \mathbf{C}_0\mathbf{Z}^\dagger\mathbf{C}_v^\dagger. \quad (\text{A9})$$

The quantity \mathbf{Z} in Eq. (A9) represents the solution to the well-known coupled-perturbed equations,²⁶ which are

$$\begin{aligned} & \mathbf{C}_v^\dagger\mathbf{F}\mathbf{C}_v\mathbf{Z} - \mathbf{Z}\mathbf{C}_0^\dagger\mathbf{F}\mathbf{C}_0 + \mathbf{C}_v(\boldsymbol{\Pi} \cdot \mathbf{P}^Z + \boldsymbol{\Omega} \cdot \mathbf{P}^Z)\mathbf{C}_0 \\ &= -\mathbf{C}_v^\dagger(\boldsymbol{\Pi} \cdot \mathbf{P}^\Delta)\mathbf{C}_0 \\ & - \frac{1}{2}\mathbf{C}_v^\dagger(\boldsymbol{\Pi}' \cdot \mathbf{R}^{I\dagger})\mathbf{C}_v\mathbf{t}^I - \frac{1}{2}\mathbf{C}_v^\dagger(\boldsymbol{\Pi}' \cdot \mathbf{R}^{J\dagger})\mathbf{C}_v\mathbf{t}^J \\ & + \frac{1}{2}\mathbf{t}^J\mathbf{C}_0^\dagger(\boldsymbol{\Pi}' \cdot \mathbf{R}^{I\dagger})\mathbf{C}_0 + \frac{1}{2}\mathbf{t}^I\mathbf{C}_0^\dagger(\boldsymbol{\Pi}' \cdot \mathbf{R}^{J\dagger})\mathbf{C}_0. \end{aligned} \quad (\text{A10})$$

(The prime in $\boldsymbol{\Pi}'$ indicates that the Coulomb contribution to the electron repulsion integrals vanishes in SF-CIS, due to $\alpha \rightarrow \beta$ excitation.)

Equation (A10) contains transition amplitudes for both electronic states, but for $I = J$ it is equivalent to the usual coupled-perturbed equations that must be solved to obtain the relaxed density $\mathbf{P}^\Delta + \mathbf{P}^Z$ and therefore the excited-state CIS analytic gradient.^{27,51} Evaluation of the difference gradient \mathbf{g}^{IJ} already requires solution of Eq. (A10) for both states (i.e., for two different vectors \mathbf{Z}), and evaluation of \mathbf{h}^{IJ} requires solution of this equation for a third \mathbf{Z} -vector with $I \neq J$ in Eq. (A10). However, all three \mathbf{Z} -vectors can be obtained simultaneously in the same set of Davidson iterations, and in our experience this typically requires only one or two iterations beyond what is required for a CIS gradient evaluation. Relative to the cost of a CIS (or TDDFT) gradient evaluation, the additional cost for derivative couplings is extremely low.

Finally, Eq. (A1) can be rewritten as

$$h_x^{IJ} = \mathbf{P}' \cdot \mathbf{H}^{[x]} + \boldsymbol{\Gamma}_1 \cdot \boldsymbol{\Pi}^{[x]} + \boldsymbol{\Gamma}_2 \cdot \boldsymbol{\Pi}'^{[x]} + \mathbf{W}' \cdot \mathbf{S}^{[x]}, \quad (\text{A11})$$

where

$$\mathbf{P}' = \mathbf{P}^\Delta + \mathbf{P}^Z, \quad (\text{A12})$$

$$\boldsymbol{\Gamma}_1 = \mathbf{P}' \otimes \mathbf{P}, \quad (\text{A13})$$

$$\boldsymbol{\Gamma}_2 = \mathbf{R}^{I\dagger} \otimes \mathbf{R}^J, \quad (\text{A14})$$

$$\mathbf{W}' = -\frac{1}{2}\boldsymbol{\Lambda}'\mathbf{C}\mathbf{C}^\dagger - \frac{1}{2}\mathbf{C}\mathbf{C}^\dagger\boldsymbol{\Lambda}'^\dagger, \quad (\text{A15})$$

$$\boldsymbol{\Lambda}' = \mathbf{P}'\mathbf{F} + \mathbf{P}(\boldsymbol{\Pi} \cdot \mathbf{P}')$$

$$\begin{aligned} & + \frac{1}{2}\mathbf{R}^I(\boldsymbol{\Pi}' \cdot \mathbf{R}^{J\dagger}) + \frac{1}{2}\mathbf{R}^J(\boldsymbol{\Pi}' \cdot \mathbf{R}^{I\dagger}) \\ & + \frac{1}{2}\mathbf{R}^{I\dagger}(\boldsymbol{\Pi}' \cdot \mathbf{R}^J) + \frac{1}{2}\mathbf{R}^{J\dagger}(\boldsymbol{\Pi}' \cdot \mathbf{R}^I). \end{aligned} \quad (\text{A16})$$

2. Derivation of h_x^{IJ} for collinear SF-TDDFT

In Ref. 34, the quantity h_x^{IJ} was derived for spin-conserving TDDFT within the TDA, based on an *ad hoc* extension of the CIS formalism. The collinear SF-TDDFT counterpart of this quantity is even simpler because $\langle a_j | \hat{\xi}_{xc} | i b \rangle$ vanishes in Eq. (30). Thus, h_x^{IJ} for SF-TDDFT is very similar to that in SF-CIS, except that $\boldsymbol{\Pi}$ is now defined according to

$$\Pi_{\mu\nu,\lambda\sigma} = \langle \mu\lambda | \nu\sigma \rangle - C_{\text{HF}} \langle \mu\lambda | \sigma\nu \rangle, \quad (\text{A17})$$

and in addition there are some additional terms arising from the orbital response of the exchange-correlation part of the Kohn-Sham Fock matrix, \mathbf{F}_{xc} .

The coupled perturbed equations now read

$$\begin{aligned} & \mathbf{C}_v^\dagger\mathbf{F}\mathbf{C}_v\mathbf{Z} - \mathbf{Z}\mathbf{C}_0^\dagger\mathbf{F}\mathbf{C}_0 + \mathbf{C}_v(\boldsymbol{\Pi} \cdot \mathbf{P}^Z + \boldsymbol{\Omega} \cdot \mathbf{P}^Z)\mathbf{C}_0 \\ &= -\mathbf{C}_v^\dagger(\boldsymbol{\Pi} \cdot \mathbf{P}^\Delta + \boldsymbol{\Omega} \cdot \mathbf{P}^\Delta)\mathbf{C}_0 \\ & - \frac{1}{2}\mathbf{C}_v^\dagger(\boldsymbol{\Pi}' \cdot \mathbf{R}^{I\dagger})\mathbf{C}_v\mathbf{t}^I - \frac{1}{2}\mathbf{C}_v^\dagger(\boldsymbol{\Pi}' \cdot \mathbf{R}^{J\dagger})\mathbf{C}_v\mathbf{t}^J \\ & + \frac{1}{2}\mathbf{t}^J\mathbf{C}_0^\dagger(\boldsymbol{\Pi}' \cdot \mathbf{R}^{I\dagger})\mathbf{C}_0 + \frac{1}{2}\mathbf{t}^I\mathbf{C}_0^\dagger(\boldsymbol{\Pi}' \cdot \mathbf{R}^{J\dagger})\mathbf{C}_0, \end{aligned} \quad (\text{A18})$$

where

$$\Omega_{\mu\nu,\lambda\sigma} = \frac{\partial F_{xc,\mu\nu}}{\partial P_{\lambda\sigma}}. \quad (\text{A19})$$

The final expression for h_x^{IJ} in collinear SF-TDDFT is

$$\begin{aligned} h_x^{IJ} &= \mathbf{P}' \cdot \mathbf{H}^{[x]} + \boldsymbol{\Gamma}_1 \cdot \boldsymbol{\Pi}^{[x]} + \boldsymbol{\Gamma}_2 \cdot \boldsymbol{\Pi}'^{[x]} \\ & + \mathbf{W}' \cdot \mathbf{S}^{[x]} + \mathbf{P}' \cdot \mathbf{F}_{xc}^{[x]}, \end{aligned} \quad (\text{A20})$$

where

$$\mathbf{W}' = -\frac{1}{2}\boldsymbol{\Lambda}'\mathbf{C}\mathbf{C}^\dagger - \frac{1}{2}\mathbf{C}\mathbf{C}^\dagger\boldsymbol{\Lambda}'^\dagger \quad (\text{A21})$$

and

$$\begin{aligned} \boldsymbol{\Lambda}' &= \mathbf{P}'\mathbf{F} + \mathbf{P}(\boldsymbol{\Pi} \cdot \mathbf{P}' + \boldsymbol{\Omega} \cdot \mathbf{P}') \\ & + \frac{1}{2}\mathbf{R}^I(\boldsymbol{\Pi}' \cdot \mathbf{R}^{J\dagger}) + \frac{1}{2}\mathbf{R}^J(\boldsymbol{\Pi}' \cdot \mathbf{R}^{I\dagger}) \\ & + \frac{1}{2}\mathbf{R}^{I\dagger}(\boldsymbol{\Pi}' \cdot \mathbf{R}^J) + \frac{1}{2}\mathbf{R}^{J\dagger}(\boldsymbol{\Pi}' \cdot \mathbf{R}^I). \end{aligned} \quad (\text{A22})$$

Other matrices have the same definitions as those in SF-CIS, except for $\mathbf{F}_{xc}^{[x]}$, which is defined as

$$\begin{aligned} F_{xc,\mu\nu}^{[x]} &= \int \frac{\partial f_{xc}}{\partial \rho} \frac{\partial \rho}{\partial P_{\mu\nu}} d\mathbf{r} + \int \frac{\partial f_{xc}}{\partial \rho} \left(\frac{\partial \rho}{\partial P_{\mu\nu}} \right)^{[x]} d\mathbf{r} \\ & + \int \frac{\partial^2 f_{xc}}{\partial \rho \partial \rho'} \frac{\partial \rho}{\partial P_{\mu\nu}} \rho^{[\bar{x}]} d\mathbf{r}. \end{aligned} \quad (\text{A23})$$

Note that within this particular SF-TDDFT formalism, third functional derivatives of f_{xc} are not required in order to compute derivative couplings.

¹J. C. Tully, *J. Chem. Phys.* **137**, 22A301 (2012).

²D. R. Yarkony, *Rev. Mod. Phys.* **68**, 985 (1996).

³B. H. Lengsfeld III, P. Saxe, and D. R. Yarkony, *J. Chem. Phys.* **81**, 4549 (1984).

- ⁴P. Saxe, B. H. Lengsfeld III, and D. R. Yarkony, *Chem. Phys. Lett.* **113**, 159 (1985).
- ⁵B. H. Lengsfeld III and D. R. Yarkony, *J. Chem. Phys.* **84**, 348 (1986).
- ⁶H. Lischka, M. Dallos, P. G. Szalay, D. R. Yarkony, and R. Shepard, *J. Chem. Phys.* **120**, 7322 (2004).
- ⁷E. Tapavicza, G. D. Bellchambers, J. C. Vincent, and F. Furche, *Phys. Chem. Chem. Phys.* **15**, 18336 (2013).
- ⁸T. Ichino, J. Gauss, and J. F. Stanton, *J. Chem. Phys.* **130**, 174105 (2009).
- ⁹A. Tajti and P. G. Szalay, *J. Chem. Phys.* **131**, 124104 (2009).
- ¹⁰V. Chernyak and S. Mukamel, *J. Chem. Phys.* **112**, 3572 (2000).
- ¹¹R. Send and F. Furche, *J. Chem. Phys.* **132**, 044107 (2010).
- ¹²I. Tavernelli, B. F. E. Curchod, A. Laktionov, and U. Rothlisberger, *J. Chem. Phys.* **133**, 194104 (2010).
- ¹³S. Fatehi, E. Alguire, Y. Shao, and J. E. Subotnik, *J. Chem. Phys.* **135**, 234105 (2011).
- ¹⁴B. G. Levine, C. Ko, J. Quenneville, and T. J. Martínez, *Mol. Phys.* **104**, 1039 (2006).
- ¹⁵S. Yang and T. J. Martínez, "Ab initio multiple spawning: First principles dynamics around conical intersections," in *Conical Intersections: Theory, Computation, and Experiment*, Advanced Series in Physical Chemistry Vol. 17, edited by W. Domcke, D. R. Yarkony, and H. Köppel (World Scientific, 2011), pp. 347–374.
- ¹⁶A. I. Krylov, *Chem. Phys. Lett.* **338**, 375 (2001).
- ¹⁷Y. Shao, M. Head-Gordon, and A. I. Krylov, *J. Chem. Phys.* **118**, 4807 (2003).
- ¹⁸Y. Yamaguchi, Y. Osamura, J. D. Goddard, and H. F. Schaefer III, *A New Dimension to Quantum Chemistry: Analytic Derivative Methods in Ab Initio Molecular Electronic Structure Theory* (Oxford University Press, New York, 1994).
- ¹⁹N. Minezawa and M. S. Gordon, *J. Phys. Chem. A* **113**, 12749 (2009).
- ²⁰N. Minezawa and M. S. Gordon, *J. Phys. Chem. A* **115**, 7901 (2011).
- ²¹N. Minezawa and M. S. Gordon, *J. Chem. Phys.* **137**, 034116 (2012).
- ²²Y. Harabuchi, S. Maeda, T. Taketsugu, N. Minezawa, and K. Morokuma, *J. Chem. Theory Comput.* **9**, 4116 (2013).
- ²³X. Zhang and J. M. Herbert, *J. Phys. Chem. B* **118**, 7806 (2014).
- ²⁴Z. Li and W. Liu, *J. Chem. Phys.* **141**, 014110 (2014).
- ²⁵D. Maurice and M. Head-Gordon, *Int. J. Quantum Chem.* **56**, 361 (1995).
- ²⁶J. A. Pople, R. Krishnan, H. B. Schegel, and J. S. Binkley, *Int. J. Quantum Chem. Symp.* **13**, 225 (1979).
- ²⁷J. B. Foresman, M. Head-Gordon, J. A. Pople, and M. J. Frisch, *J. Phys. Chem.* **96**, 135 (1992).
- ²⁸R. M. Shroll and W. D. Edwards, *Int. J. Quantum Chem.* **56**, 395 (1995).
- ²⁹J. B. Delos, *Rev. Mod. Phys.* **53**, 287 (1981).
- ³⁰D. R. Yarkony, *J. Chem. Phys.* **84**, 3206 (1986).
- ³¹W. Kutzelnigg, *Mol. Phys.* **105**, 2627 (2007).
- ³²S. Fatehi and J. E. Subotnik, *J. Phys. Chem. Lett.* **3**, 2039 (2012).
- ³³F. Wang and T. Ziegler, *J. Chem. Phys.* **121**, 12191 (2004).
- ³⁴Q. Ou, S. Fatehi, E. Alguire, Y. Shao, and J. E. Subotnik, *J. Chem. Phys.* **141**, 024114 (2014).
- ³⁵S. Hirata and M. Head-Gordon, *Chem. Phys. Lett.* **314**, 291 (1999).
- ³⁶M. Huix-Rotllant, B. Natarajan, A. Ipatov, C. M. Wawire, T. Deutsch, and M. E. Casida, *Phys. Chem. Chem. Phys.* **12**, 12811 (2010).
- ³⁷Y. Shao, L. Fusti-Molnar, Y. Jung, J. Kussmann, C. Ochsenfeld, S. T. Brown, A. T. B. Gilbert, L. V. Slipchenko, S. V. Levchenko, D. P. O'Neill, R. A. DiStasio Jr., R. C. Lochan, T. Wang, G. J. O. Beran, N. A. Besley, J. M. Herbert, C. Y. Lin, T. Van Voorhis, S. H. Chien, A. Sodt, R. P. Steele, V. A. Rassolov, P. E. Maslen, P. P. Korambath, R. D. Adamson, B. Austin, J. Baker, E. F. C. Byrd, H. Dachsel, R. J. Doerksen, A. Dreuw, B. D. Dunietz, A. D. Dutoi, T. R. Furlani, S. R. Gwaltney, A. Heyden, S. Hirata, C.-P. Hsu, G. Kedziora, R. Z. Khalliulin, P. Klunzinger, A. M. Lee, M. S. Lee, W. Liang, I. Lotan, N. Nair, B. Peters, E. I. Proynov, P. A. Pieniazek, Y. M. Rhee, J. Ritchie, E. Rosta, C. D. Sherrill, A. C. Simmonett, J. E. Subotnik, H. L. Woodcock III, W. Zhang, A. T. Bell, A. K. Chakraborty, D. M. Chipman, F. J. Keil, A. Warshel, W. J. Hehre, H. F. Schaefer III, J. Kong, A. I. Krylov, P. M. W. Gill, and M. Head-Gordon, *Phys. Chem. Chem. Phys.* **8**, 3172 (2006).
- ³⁸A. I. Krylov and P. M. W. Gill, *WIREs Comput. Mol. Sci.* **3**, 317 (2013).
- ³⁹See supplementary material at <http://dx.doi.org/10.1063/1.4891984> for finite-difference results that provide evidence for the correctness of the analytic implementation.
- ⁴⁰S. Gozem, F. Melaccio, A. Valentini, M. Filatov, M. Huix-Rotllant, N. Ferré, L. M. Frutos, C. Angeli, A. I. Krylov, A. A. Granovsky, R. Lindh, M. Olivucci, *J. Chem. Theory Comput.* **9**, 284 (2014).
- ⁴¹A. D. Becke, *Phys. Rev. A* **38**, 3098 (1988).
- ⁴²C. Lee, W. Yang, and R. G. Parr, *Phys. Rev. B* **37**, 785 (1988).
- ⁴³M. Barbatti, J. Paier, and H. Lischka, *J. Chem. Phys.* **121**, 11614 (2004).
- ⁴⁴M. J. Bearpark, M. A. Robb, and H. B. Schlegel, *Chem. Phys. Lett.* **223**, 269 (1994).
- ⁴⁵S. Maeda, K. Ohno, and K. Morokuma, *J. Chem. Theory Comput.* **6**, 1538 (2010).
- ⁴⁶B. G. Levine, J. D. Coe, and T. J. Martínez, *J. Phys. Chem. B* **112**, 405 (2008).
- ⁴⁷J. S. Sears, C. D. Sherrill, and A. I. Krylov, *J. Chem. Phys.* **118**, 9084 (2003).
- ⁴⁸Z. Li, W. Liu, Y. Zhang, and B. Suo, *J. Chem. Phys.* **134**, 134101 (2011).
- ⁴⁹D. Casanova and M. Head-Gordon, *J. Chem. Phys.* **129**, 064104 (2008).
- ⁵⁰Y. A. Bernard, Y. Shao, and A. I. Krylov, *J. Chem. Phys.* **136**, 204103 (2012).
- ⁵¹F. Liu, Z. Gan, Y. Shao, C.-P. Hsu, A. Dreuw, M. Head-Gordon, B. T. Miller, B. R. Brooks, J.-G. Yu, T. R. Furlani, and J. Kong, *Mol. Phys.* **108**, 2791 (2010).